

A dynamic mechanical analysis of the interfacial changes induced from both the reinforcement and the matrix sides in polypropylene/surface modified talc composites

Jesús María García-Martínez, Jesús Taranco, Susana Areso, Emilia P. Collar

Grupo de Ingeniería de Polímeros, Instituto de Ciencia y Tecnología de Polímeros, C.S.I.C., C/Juan de la Cierva 3, 28006 Madrid, Spain

Correspondence to: J. M. García-Martínez (E-mail: jesus.maria@ictp.csic.es)

ABSTRACT: The interfacial changes associated with a series of polypropylene based composite materials with modified interphases from the reinforcement side, from the matrix side and both were studied by following their dynamic mechanical behavior. Composites consisted in an isotactic polypropylene (iPP) matrix, a series of talc with different surface functionalities (hydroxyl, chloride, *n*-butyl amine, and silanes) and a commercial interfacial agent from the matrix side (iPP-SA with 5% of grafts). A comprehensive interpretation of the link existing between the dynamic mechanical responses of the series of 75/25 iPP/talc composites and the molecular relaxation spectrum occurring in the polymer phase of the composites is made with emphasis on the role played by the interfacial modifications performed from each and both sides of the interphase. Dynamic mechanical analysis has been used here to study how the intended interfacial modifications affected the behavior of the composites. The efficiency of the interfacial phenomena is discussed from a phenomenological point of view as well as by considering classical criteria such as the glass transition temperature and the glass to rubbery transition. Finally, a correlation between mechanical parameters from the microscopic scale and others from the macroscopic scale appears to emerge. © 2015 Wiley Periodicals, Inc. *J. Appl. Polym. Sci.* **2015**, *132*, 42678.

KEYWORDS: DMA; interfacial modifications; interfacial modifiers; interphase; iPP/talc composites; modified talc

Received 26 March 2015; accepted 29 June 2015

DOI: 10.1002/app.42678

INTRODUCTION

Composites based on isotactic polypropylene (iPP) and talc have been being studied since many years ago,^{1–15} but however and despite the time elapsed since early works, it is an actual topic.^{12–19} In this work, it is proposed that an interfacial modification significant enough as to be detected at the macroscopic scale also must be found at the subsequent micro, meso, and nano scales, particularly as it is in the nano meter domain where the interfacial changes take place. It is based on previous works by the authors where the interfacial modifications in polypropylene/talc composites were detected and explained by following their macroscopic responses. These were detected both at room temperature under normal stresses and controlled testing rates (tensile and flexural modes), as well as under instantaneous testing rates (impact mode), both well below and above the matrix glass transition temperature.^{7–10} As the reinforcement, lamellar talc was chosen because it has proved to ensure the no breakage of their particles all along the processing steps in previous works by the authors.^{7–11,13–15} This was done to avoid common misinterpretations in considering due to interfacial modifications, the changes

in the composites performance merely due to the changes in particle size causing the interfacial area to increase with the decrease in the particle size of the reinforcement.

The efficiency of the surface treatments of the talc particles was ascertained at the macroscopic scale. Treatments on the mineral particles were performed, on one hand, by removing the hydroxyl groups present on the particle surface by means of a chemisorption reaction set and, on the other hand, by following different physisorption processes looking for the mere coating of the talc particles by moieties able to enhance the polypropylene/talc affinity.^{11,13–15}

From the experimental result fits in previous works by the authors, by following the Box–Wilson surface response methodology it was possible to determine that the matrix/reinforcement 75 : 25 ratio was the critical compositional value to maximize the response area of the composites. The latter was performed under different external stimuli, mainly from mechanical and/or thermal fields. Further, it was ascertained that the substitution of just a small amount (such as 1.5%, w/w) of the polypropylene matrix by a commercial succinic anhydride grafted isotactic

Table I. Physical Properties of the Polymers Used in the Composites Manufacture

Sample	M_w	M_n	M_w/M_n	ρ (kg/m ³)	T_m (°C)	T_c (°C)	λ_m (%)	λ_c (%)
iPP ^a	334,400	59,500	5.6	901	164.0	117.5	41.8	41.9
iPP-SA ^b	69,000	3900	17.7	900	159.0	98.5	40.5	42.5

^a Neat polypropylene.^b Interfacial agent.

polypropylene (iPP-SA) with 5% of grafted groups, was not only enough but necessary to maximize the interaction level between the polypropylene matrix and the talc particles.^{7–10}

According to those findings, the dynamic mechanical analysis (DMA) results discussed in this work correspond to the 75/25, w/w, iPP/talc system, pristine, and with modified interfaces from either as both the matrix and the reinforcement sides. The modifications from the reinforcement side were performed by two differenced ways. On one hand, a series of surface modified talc were obtained by removing, through gas/solid, or vapor/solid chemisorptions reactions, the surface hydroxyl groups, and substituting them for either chloride or ammonia groups and, on the other hand, by the physisorption treatment of the talc particles with either *n*-butyl-amine, or silane. A DMA study on the behavior of composites with solely interfacial modifications from the reinforcement side was published by authors.¹³ This work continues the latter studies by exploring the possibilities of DMA to ascertain the interfacial changes in the 75/25 iPP/Talc modified composites from both the matrix and the reinforcement sides. Basic parameters, such as the glass transition temperature of the matrix and the ratio between the values of the DMA parameters in the glassy and the rubbery regions, are also considered. Finally, a correlation between the tensile modulus of the composites at the macroscopic scale and the DMA storage modulus is shown.

EXPERIMENTAL

Materials

An isotactic polypropylene (iPP), Isplen 050, supplied by Repsol S.A., was used as the polymer matrix in the composites. The interfacial agent used was a commercial isotactic polypropylene with maleic anhydride grafted moieties (iPP-SA). The grafting degree of the latter was 5%, w/w (5×10^{-4} mol/g). Table I lists some properties of both the polymer matrix and the interfacial agent.

The lamellar talc used was supplied by Luzenac, ($\rho = 2750$ kg/m³; BET = 5.3 m²/g; mean particle size = 10.1 μ m). A series of lamellar talc with modified surfaces were obtained in the authors' labs. Two of them, named talc-Cl and talc-NH_{2(g)} were obtained by gas/solid chemisorption reactions yielding modified talc with chlorine, or ammonia groups bonded on the talc surface instead of their original hydroxyl groups. The third modified talc: talc-NH_{2(v)}, was obtained by a vapor/solid chemisorption reactions. Finally, the fourth and fifth modified talc were obtained by classical physisorption liquid/solid treatments of the talc particles with silane or *n*-butyl-amine, and named as talc-silane or talc-nBuNH₂, respectively. The details about the talc modification

processes are beyond the scope of this work and were fully described previously.^{10,11,13,14}

Processing

All the 75/25 iPP/talc composites were obtained by mixing the components in a counter-rotating twin screw extruder Collin[®] ZK25 type. As the interfacial modifier from the matrix side, iPP-SA, was added by substituting 1.5%, w/w of the polypropylene matrix; the premixed dry blend was feed to the extruder. The extruder screw design, with an adequate *L/D* ratio (*L/D* = 18), ensured the uniform distribution of the talc particles which were feed from the vacuum section into the iPP molten matrix. The temperature profile of the extruder was set as 200; 210; 210; and 220°C, with a die temperature of 230°C and a screw speed set at 85 rpm for a throughput of 10 kg/h. After cooling in a water bath, the filament was pelletized by a Dr. Collin GmbH pelletizer. To safeguard the effect of processing conditions on the response levels of the polypropylene, the pristine components were extruded, pelletized, and compression molded under the same set conditions as those of the iPP/talc composites. A polypropylene compound incorporating 1.5% of the interfacial modifier, iPP-SA, was also processed.

The pellets of the different compounds were compression molded into 120 × 120 × 4 mm³ sheets in a Collin[®] Press (Germany) 200 × 200 model, with a plate temperature of 180°C. A two step pressure cycle (2 and 3 min, respectively) of 3.3 MPa was done to ensure softening of the material and then correct packing. The mold was then introduced into a water cooled cartridge, maintaining pressure, until cooled to room temperature. The molding process was chosen to minimize (as far as possible) additional effects on the final properties due to preferential orientations inside the samples and maximize those effects due to the influence of the interfacial changes. The sheets were always verified to be free of defects such as bubbles, warpage, holes, and so forth. Finally, the samples were conditioned at room temperature and 50% R.H for at least 48 h prior to be machined according to the DMA testing specifications.

Characterization

The mineral content was determined by thermo-gravimetric analysis (TGA) under N₂ atmosphere and dynamic heating (10°C/min) using a TA Instruments, Q50 Thermal Analyzer. The results showed that the mineral content in all the samples were in the 24.9 ± 0.2 range, corroborating those previously determined by ash content after pyrolysis at 900°C.^{11,13–15}

DMA tests under reverse loading mode were performed in a TA Instruments 983 model, Dynamic Mechanical Spectrometer. Specimen dimensions were 21.2 × 10.4 × 4 mm³. The test frequency and oscillation amplitude were fixed at 1 Hz and 0.2 mm, respectively,

Table II. Thermal Parameters (DSC) of the Indicated Samples

Sample	T_m (°C)	T_c (°C)	λ_m (%)	λ_c (%)
iPP	164.0	123.0	27.0	24.8
iPP/ iPP-SA	164.5	122.8	40.1	41.2
iPP/Talc ^a	164.0	122.5	42.2	43.8
iPP/Talc/iPP-SA ^a	164.3	133.3	48.0	47.8

^aWith original (unmodified) talc.

with a clamping distance of 14.5 mm. Thermal scanning was from -30 up to 150°C at a heating rate of $2^\circ\text{C}/\text{min}$. The rather low frequency used and the applied displacements were chosen to avoid nonlinear responses and morphological changes caused by internal heat generation. For all the compounds considered in this work, the in-phase storage modulus (G'), the out-of-phase loss modulus (G'') and the loss, or damping factor ($\tan \delta = G''/G'$) as a function of temperature, were recorded.

Tensile test for elastic modulus (E) calculations was performed at room temperature (23°C) using an Instron 4200 dynamometer equipped with a high resolution extensometer (HDR) by following ISO 527-1/2 standards. The crosshead speed was 1.0 mm/min, and at least five specimens of each composite were tested.¹⁰

Additionally, differential scanning calorimetry (DSC) was performed on chosen samples using a Perkin-Elmer DSC-7. Tests were performed on standard crucibles containing around 10 mg of sample, from 40°C up to 200°C and reverse, under nitrogen atmosphere and at heating/cooling rates of $10^\circ\text{C}/\text{min}$. After the first heating step, the sample was held for 5 min in the molten state, and then the cooling step was recorded, ending the test with a second heating step with both heating steps also recorded. The full reproducibility of the thermal results was examined by testing three samples of each compound. The enthalpies associated with the corresponding melting or crystallization peaks were calculated using the DSC-7 software referred to the real amount of polymer present for each sample. The crystalline content of PP in each composite, as processed, λ_m , and from the crystallization, λ_c , was calculated from the results of the first heating scan and the cooling scan, respectively, by considering 209 J/g as the standard for 100% crystalline polypropylene.^{20–22} Table II compiles these results.

RESULTS AND DISCUSSION

It is well worth to mention, previously to discuss about the modifications observed in the properties of the composites, that the absences of changes in the mean particle size and in the particle size distribution must be checked. In this work, the mean particle size was 10.1 ± 0.1 μm for the original and all the treated talc, remaining constant even after processing as discussed previously by authors.^{11,13–15} Also, the real (and not merely the nominal) mineral content must be checked. The above-mentioned is mandatory to avoid false interpretation as interfacial phenomena the mere change in flow dynamics caused by different mineral contents. So, the only purpose of TGA in this study is to confirm the mineral content close to 25% (in our case it is in the 24.9 ± 0.2 interval). In the same way, the

thermal properties of a series of chosen samples were measured. The latter was done to obtain information about the nucleating effect caused by the presence of the odd components (talc and/or iPP-SA) in the iPP fraction of the composites.^{11,14}

The results discussed in this work deal with the study of the DMA parameters of the iPP/Talc system and the way they are influenced by the interfacial modifications performed. Figure 1 shows the evolution of the different DMA parameters with temperature for iPP and iPP/talc. Figures 2–4 show the evolution of the viscoelastic responses with temperature for the iPP/talc composites with modified interfaces from the matrix (with iPP-SA) and the reinforcement sides. For comparison reasons, these figures also include the DMA responses of the iPP/talc composites with modified interfaces from only the reinforcement side. That is, a set of iPP/chemisorption modified talc composites (iPP/talc-Cl; iPP/talc-NH_{2(g)}; iPP/talc-NH_{2(v)}), and also iPP/physisorption modified talc ones (iPP/talc-silane; iPP/talc-nBuNH₂). The description of all the modified talc used here has been fully discussed by authors' elsewhere.^{11,13,14}

This study was undertaken according three different, but complementary, criteria.^{23–26} The first criterion has a phenomenological character and follows the evolution of the different matrix parameters along the temperature axis. The second criterion is related to the mobility of the “free” polypropylene amorphous phase, and focuses in how the interfacial interactions affect to β transition peak (T_g). The third one explores the rubbery to elastic transition region between the crystalline and the “non-free” amorphous phases in the polymer matrix. It would be relevant in future works planned to assess the role played by the molding process in the polypropylene DMA responses.

Phenomenological Criterion

We consider five different intervals in the dynamic-mechanical spectra related to the relaxation and dissipation phenomena that take place when we applied oscillating forces and/or deformations, as a function of temperature, to our samples.^{13,14} The five zones are labeled in Figure 1. They show the evolution of the storage modulus (G'), loss modulus (G''), and loss, or damping factor ($\tan \delta$) with temperature for both the neat polypropylene, iPP, and the 75/25 iPP/Talc pristine composite. The first interval, between -20°C and -10°C , is characterized by being the zone where the mechanical energy dissipation capabilities of the polymer are lower. This is because they are restricted to mere short segment motions. So, variations of G' , G'' , and $\tan \delta$ with T for each one of the measured samples were not significant. The second zone considered is between -10°C and 40°C and is where the glass transition of the polymer (the β relaxation peak) occurs because short range but cooperative diffusion motions at the chain segment level occur. This zone is associated with the amorphous fraction of the isotactic iPP of the polymer matrix in the composites. The third zone is located between 40 and 80°C , and is characterized by the rubbery to elastic transition, typically characterized by a plateau region in the G'' curve for the neat iPP. This one is defined by being the zone where rapid short range diffusion motions strongly dependent on the molecular mass and the chain entanglement density take place. In this zone, a transition

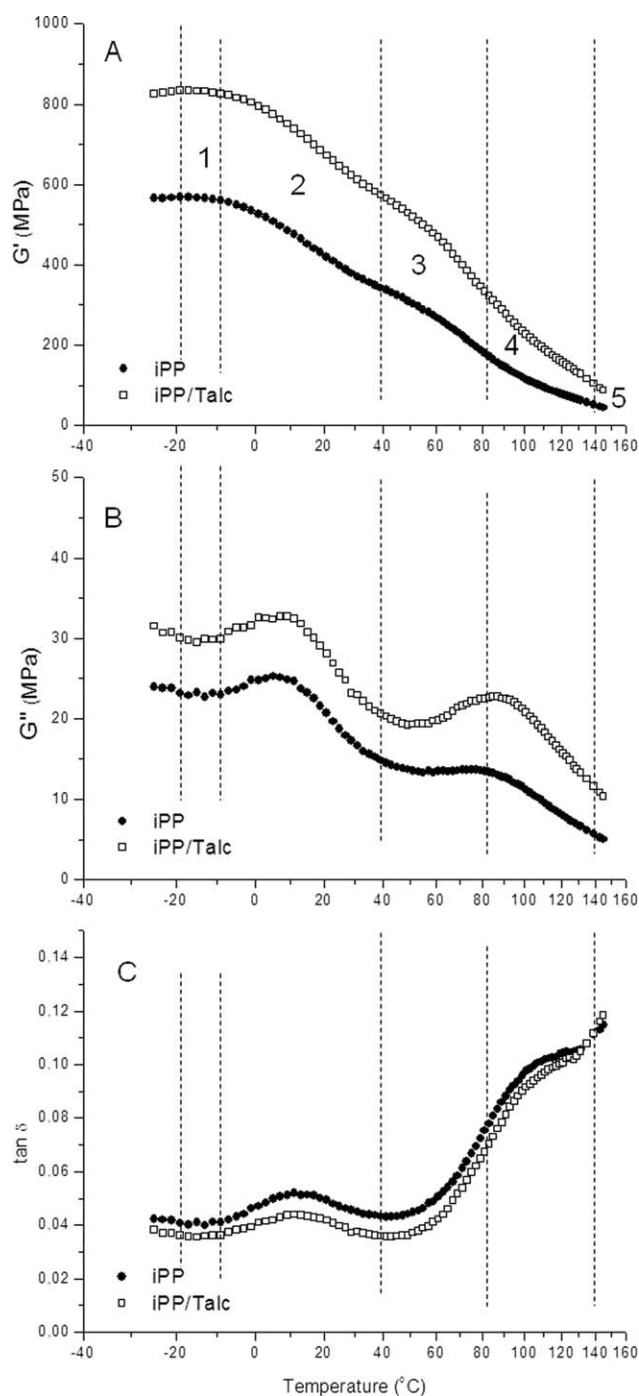


Figure 1. Evolution of the storage modulus (G'), loss modulus (G''), and loss factor ($\tan \delta$), with temperature for the neat iPP and the original iPP/Talc composite indicating the five temperature zones chosen in this work.

occurs close to 80°C (α transition) which is assigned to polymer rearrangements in the crystalline domains and across the amorphous/crystal interphase. This is driven by the so named lamellar thickening assigned to the diffusion of the conformational defects in the crystalline phase towards the “non free” amorphous phase, across the dynamic amorphous/crystal interface. Thus, the DMA responses in this area should depend not only on the amorphous to crystalline ratio in the polymer matrix of the composite, but

also on how both phases are dynamically connected.^{13,14,27} The latter strongly depends on how the polymer reached the solid state, in other words, on the molding step. The fourth interval, above 80°C up to 140°C, is where the polymer macromolecules improve greatly their capability to flow under stress and so to participate in dissipative phenomena through long range conformational changes. Finally, above 140°C a fifth interval, characterized by being the zone where the material is passing from the softening state to the molten state, can be found. In this last interval, as a consequence of the passing of the polymer to the liquid state, the tendency of the G' and G'' curves is to converge.^{13,14}

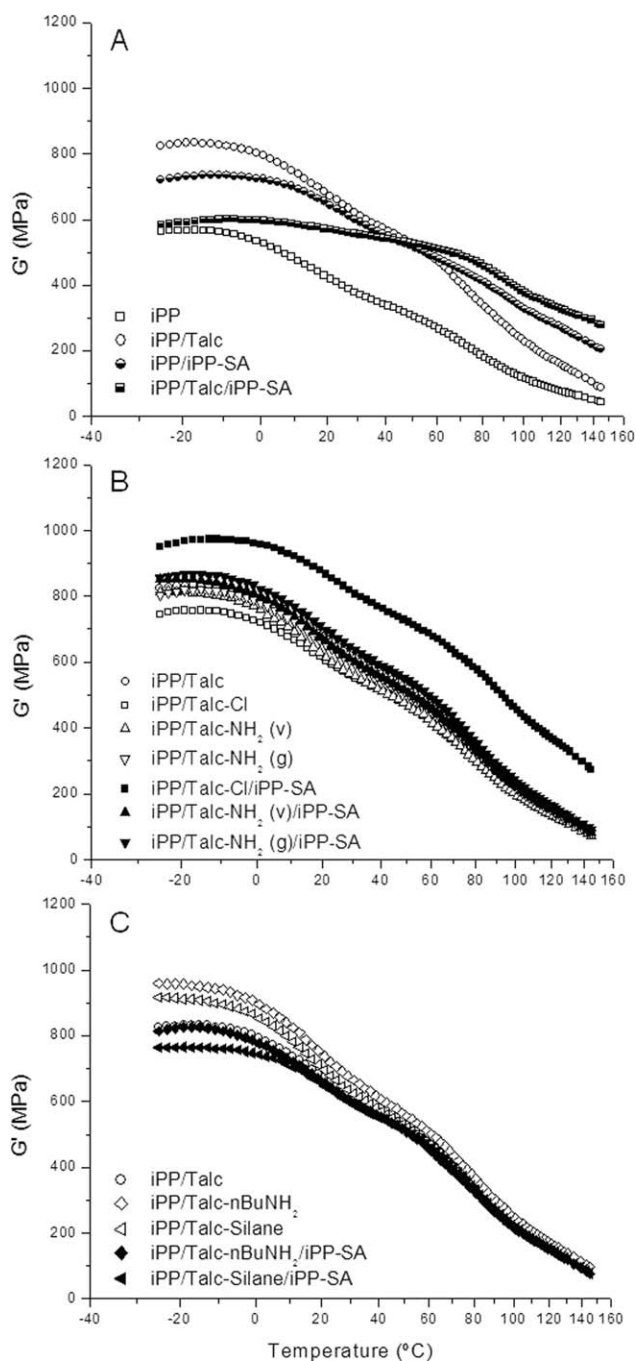


Figure 2. G' plots versus temperature for the indicated compounds.

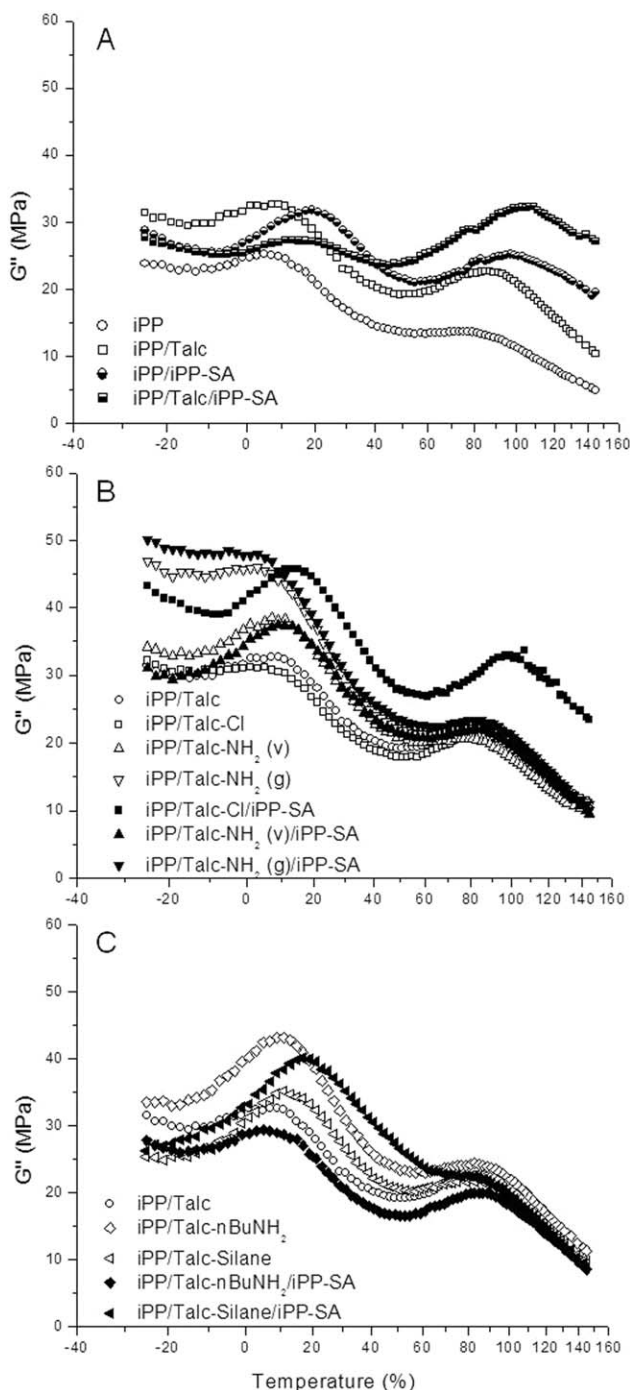


Figure 3. G'' plots versus temperature for the indicated compounds.

As mentioned above, Figure 1 shows the evolution with temperature of G' , G'' , and $\tan \delta$ for iPP and iPP/talc. The presence of the talc particles increased greatly the G' and G'' values of the composite, while its $\tan \delta$ values were below those of the neat iPP, indicating a decrease in the degree of out of phase response between the moduli. Further, while the G'' plot for iPP clearly shows a plateau region in the third temperature zone, with no evidence of the α transition peak, the G'' plot for the 75/25 iPP/talc composite shows a clear inflexion point near 60°C, which finds a correspondence with the slope change of the G' plot at this point.

This inflexion point identifies the clearly observable overlapping between the α and β transition peaks. These changes between the G'' plots of the pristine and of the semi crystalline matrix in the iPP/talc composite are suggested to be related with the higher crystalline content (λ) of the latter. In fact, the λ_m of iPP/talc was more than 50% greater than that of iPP (Table II), and is attributed here to the well known nucleating effect of the talc particles in iPP.

It is noteworthy that in the second temperature zone, corresponding to the glass transition region, both G'' plots look almost identical. In other words, the “free” amorphous phases

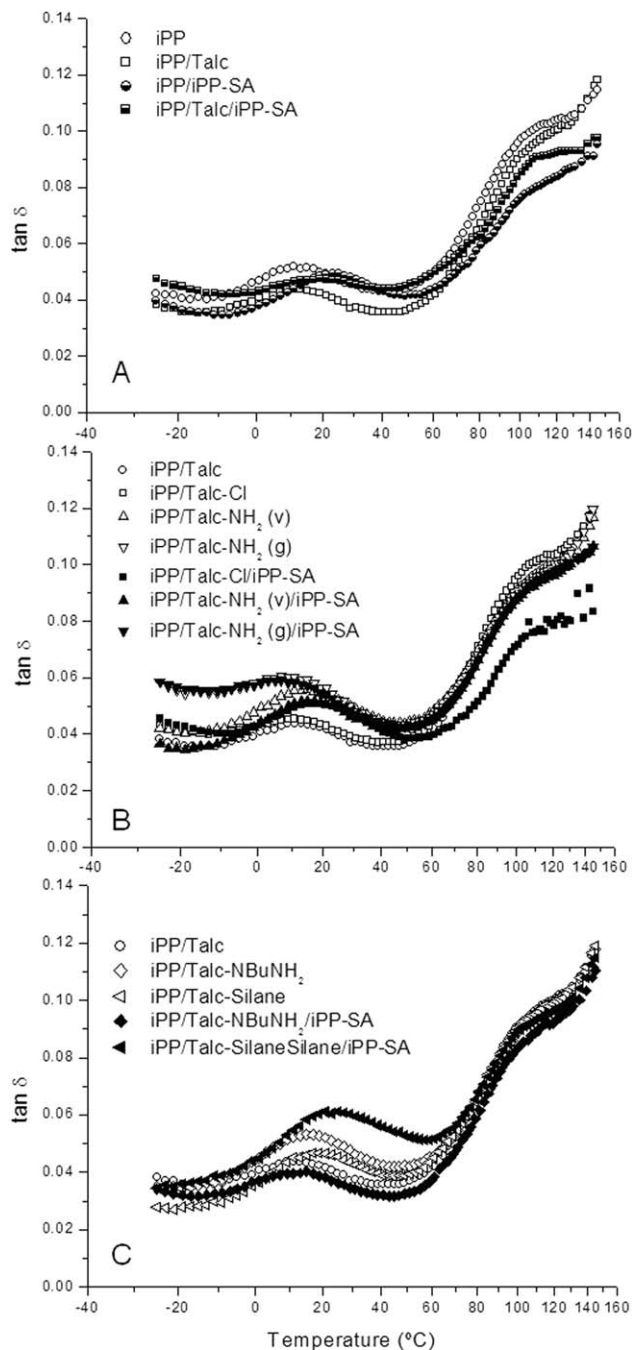


Figure 4. $\tan \delta$ plots versus temperature for the indicated compounds.

of the neat iPP and of the iPP/talc composite (responsible for the glass transition) gave rise to very similar DMA responses. In contrast, in the next temperature zone, where the α transition takes place, one finds a significant difference between the G'' plots. This is due to the fact that α transition is assigned to the amorphous/crystal interfaces and so would be informative about the highly strained and “non-free” polypropylene amorphous phase surrounding each talc particle and at the amorphous/crystal interfaces of the transcrystalline regions growing edge of the talc particles surfaces. In this sense, it is important to observe the almost identical λ_m and λ_c values for each one of the samples compiled in Table II. As the λ_c values were obtained from the cooling thermogram, after the 5 min the sample remained in the molten state, the optimal setup conditions applied in the compression molding process to all the composites studied at this work were similar, presumably resulting in non-significant changes in their crystalline contents. This was previously concluded by the authors' elsewhere.^{28,29}

Conversely, and as expected, the $\tan \delta$ evolution looks almost similar for both the iPP/talc composite and the neat iPP, with the iPP/talc slightly shifted downward. The absence of any other change in the plots let us conclude that the dissipation mechanisms are similar for both the composite and the neat iPP.

Figures 2–4, respectively, display the G' , G'' , and $\tan \delta$ plots of the samples studied in this work. Each one of the figures compiles three sets of G' , G'' , and $\tan \delta$ plots, named as A, B, and C. The A plots, in addition to the plots of the neat iPP and 75/25 iPP/talc composite, also display the DMA parameters, on one hand, of the 75/25 iPP/talc modified composite from the matrix side by the presence of 1.5% of the succinic anhydride grafted isotactic polypropylene (iPP-SA) and on the other hand, of the neat iPP just incorporating a 1.5% of the iPP-SA (iPP/iPP-SA). This amount of iPP-SA showed to be optimal to obtain the maximum of the interfacial activity when the dispersed phase is rigid.^{7–10,15} The B and C plots of Figures 2–4 show the DMA parameters for all the composites studied in this work.

Elastic Behavior. Figure 2 displays the evolution of the G' plots for all the samples studied in this work. The general conclusion is that the presence of whatever the foreign components (talc or iPP-SA) increases greatly G' of each sample with respect to that of the neat polypropylene. In Figure 2(A), it is pointed out that the values for G' in the case of the modified composite (iPP/talc/iPP-SA) at low temperatures were very similar to those of iPP, but remained almost constant up to 40°C whereas iPP decreased. Further, it is noteworthy to mention that all the G' plots of the modified compounds (iPP/talc; iPP/iPP-SA; and iPP/talc/iPP-SA) converged (exhibited the same value) close to 40°C, just the starting point of the third region of the elastic to rubbery transition zone. So, the latter appears as a reference point for a further study of the interfacial modifications. Moreover, the presence of talc or iPP-SA separately in Figure 2(A) did not appear to greatly change the G' plot evolution but the presence of both talc and iPP-SA changed abruptly the pattern of the evolution of G' with temperature. This has been more profoundly discussed elsewhere.¹⁴ In essence, that change would

be related to the dissipation mechanism by variations in the interfacial activity for those relaxations related to the “free”/“non-free” amorphous phase ratio in the iPP matrix. It is noted that the “free” amorphous phase has been defined as the portion of the amorphous PP able to become mobile in the polymer because is far enough away of those amorphous regions fully embedding the mineral particles.^{30–33}

For temperatures above 40°C, G' for the unmodified composite (iPP/Talc) increase and is closer to the G' for the neat iPP. At high temperature, G' values for iPP/talc/iPP-SA exhibit a smooth decrease, close to the G' values of the iPP/iPP-SA system above 40°C. However, at the highest temperature scanned (close to 140°C), they were in four times the values of the neat iPP, in good agreement with their differences in crystalline content as compiled in the Table II.

Figure 2(B) shows the G' plots for the 75/25 iPP/Talc composite and those incorporating just the chemisorption modified talc (open symbols) and both the 1.5% of the iPP-SA and the chemisorption modified talc (solid symbols). As it is indicated above, the open symbols curves were plotted just to ascertain the coherence of the whole study and were fully discussed elsewhere.¹³ This discussion is focused on the closed symbol plots. We observe that all the curves followed a similar pattern. Indeed, the G' plots of the both sides (of the interface) modified composites appear as almost parametric upward shift curves of the G' plot of the original 75/25 iPP/talc composites. Thus, from the evolution of G' a synergistic behavior of the combined interfacial treatments can be concluded, with the iPP/Talc-Cl/iPP-SA system being the most effective. These observations are in contrast with those relative to the Figure 2(C) which show the evolution of the G' plots of the original composite and those incorporating the physisorbed modified talc and the 1.5% of the iPP-SA as interfacial modifier. Equally to 2B, all the G' curves also exhibited a similar pattern but contrary to what happened with the chemisorption modified talc, the presence of iPP-SA here appeared to play an antagonistic effect resulting in an almost overlapping of this with the G' plot of the pristine composite above 10°C. Below this temperature and in the first temperature zone, while the G' curve of the iPP/Talc-nBuNH₂ composite remained almost overlapped with that of the pristine one, the iPP/Talc-Silane composite showed the lowest G' values of all the composites, the original iPP/talc included. By the comparison between Figure 2(B,C) it results clear that are the first and the second temperature regions of the DMA spectrum where the differences in G' of the modified composites are significant. So, the temperature response area for the glass transition is strongly affected by the amorphous phase features of the polypropylene in the composites. These include the constrained amorphous fraction just embedding each talc particle, the constrained amorphous fraction trapped at the dynamic amorphous/crystal interface, and the “free” amorphous phase responsible of the glass transition.

Viscous Behavior. Figure 3 allows a deep study of the variations in the dissipation capabilities of the amorphous phase of the modified composites with respect to the pristine one.

Table III. Transition Temperatures, Glassy to Rubber Parameters (C and C^*), and Elastic (Tensile Modulus, E , and Shear Storage Modulus, G') for the Samples Studied at This Work

Sample	$T_{\beta}^{G''}$ (°C)	$T_{\alpha}^{G''}$ (°C)	$T_{\alpha}^{G''}$ (°C)	$T_{\beta}^{\tan \delta}$ (°C)	$^a \Delta T$ (°C)	C	C^*	E (MPa)	G' (MPa)
iPP	5.0	-	-	11.3	6.3	-	-	1697	409
iPP/Talc	8.0	85.2	-	11.9	3.9	0.85	1.00	1678	635
iPP/iPP-SA	18.4	97.7	81.7	23.4	5.0	0.77	0.90	2408	654
iPP/Talc/iPP-SA	15.2	106.0	76.4	18.0	2.8	0.62	0.72	2980	570
iPP/Talc-Cl	4.7	82.8	-	11.3	6.6	0.87	1.02	2293	590
iPP/Talc-Cl/iPP-SA	14.5	96.3	63.8	17.4	2.9	0.73	0.85	2200	600
iPP/Talc-NH _{2(v)}	8.5	79.8	-	14.0	5.5	0.93	1.08	2243	641
iPP/Talc-NH _{2(v)} /iPP-SA	10.0	84.0	-	14.0	4.0	0.89	1.05	2836	790
iPP/Talc-NH _{2(g)}	4.9	79.2	-	10.6	5.7	0.87	1.02	3453	648
iPP/Talc-NH _{2(g)} /iPP-SA	5.0	82.8	-	10.0	5.0	0.85	1.00	3592	688
iPP/Talc-nBuNH ₂	9.6	84.0	-	15.3	5.7	0.91	1.06	3011	720
iPP/Talc-nBuNH ₂ /iPP-SA	4.0	81.7	65.0	12.0	6.0	0.87	1.02	2583	680
iPP/Talc-Silane	11.2	84.0	-	17.4	6.2	0.96	1.06	2914	643
iPP/Talc-Silane/iPP-SA	17.5	84.0	-	20.8	3.3	0.81	0.95	2809	636

$$^a \Delta T = [T_{\beta}^{\tan \delta} / T_{\beta}^{G''}].$$

Figure 3(A) shows the G'' curves for the iPP, the pristine 75/25 iPP/talc, the iPP/iPP-SA compound, and the iPP/talc/iPP-SA modified composite. In a similar manner that the presence of talc in the iPP matrix shifted the G'' curve to higher values with respect to that of the neat iPP and made appear a clear α transition peak (that almost disappeared in the subtle plateau region at the G'' curve for the neat iPP), the G'' plots of the modified composite (iPP/Talc/iPP-SA) and of the iPP/iPP-SA system also displayed their respective α transition peak. In addition they exhibit a clear shoulder placed around 80°C. Moreover, both the β and the α transition peaks of both of the latter samples appeared clearly shifted to higher temperatures with respect to those of the neat iPP and the pristine composite. Table III lists the corresponding peak temperatures for the β and α transitions in these plots. With respect to those from the G'' plots displayed in Figure 3(A), increases in the T_{β} peak by the presence of the iPP-SA of 13 and 7°C for, respectively, the neat iPP and the 75/25 iPP/talc can be observed. Both values are larger than that of that of 3°C above the T_{β} peak value of the pristine composite with respect to that of the neat iPP, because of the higher PP crystalline content in the composite. Thus, both large increases would agree with a higher energy level need for the glass transition may occur in the “free” amorphous fraction of the iPP. In such sense, it is also noteworthy to mention the lower area under the β peak of the modified composite (iPP/Talc/iPP-SA) than that under the β peak of iPP/iPP-SA compound. It would evidence a significant reduction in the “free” amorphous fraction of the iPP able to participate in the glass transition because of the higher interaction level at the iPP/talc interface promoted by the SA polar groups grafted in the interfacial modifier from the matrix side. The large increase in the energy threshold needed to start the main dissipation mechanisms assigned to the amorphous fractions in the iPP, by the presence of iPP-SA at its optimal amount, is also put into evidence by the 12.5 and 20°C increases in the α transition

peak, respectively, observed for the iPP/iPP-SA compound and the iPP-SA modified composite (iPP/Talc/iPP-SA). In addition, the latter appears to be confirmed by the presence of a little shoulder in both α peaks (α' , $T_{\alpha'}$ in Table III, which agrees with the secondary crystallization processes occurring in chemically modified isotactic polypropylenes with grafted polar monomers.^{14,28,29}

Indeed, from the previous discussion over the G' plots in Figure 2(A), the effective role of the iPP-SA as a true interfacial modifier was concluded. It means that the iPP-SA (because the SA groups are rejected from the iPP bulk)^{14,28,29} is placed at the iPP/talc interface and is trapped between the trans-crystalline regions formed by the iPP matrix and their corresponding highly constrained amorphous segments embedding each talc particle. Because of being semi-crystalline too, further due to its lower molecular sizes than those of the iPP matrix (Table I), the crystalline regions of the highly constrained iPP-SA bring their own response to the overall lamellar thickening process assigned to the diffusion of the conformational defects in the crystalline phase towards that “non free” amorphous phase, across the dynamic amorphous/crystal interface. This interpretation is confirmed by observing that the same response is found in the absence of the talc particles; by the presence of 1.5% of the iPP-SA in the iPP. This is placed in the same free volume fraction of the iPP bulk, as deduced from the almost identical crystalline level as that in the 75/25 iPP/talc composite (Table II), but with a significant population of “free” amorphous phase able to participate in the glass transition [respective to that existing in the modified composite, as deduced from the comparison of the β peak areas comparison in the Figure 3(A)].

In Figure 3(B,C), the composites modified from both sides of the iPP/talc interface can be observed. The open symbols curves that were discussed elsewhere¹³ are reproduced here, on one hand, to allow observe at a glance that the chemisorption modified talc

composites show different G'' responses when iPP-SA is present. On the other hand, and in contrast with the pristine composite, it is noteworthy that both the composites incorporating the surface aminated talc (iPP/Talc-NH_{2(v)}) and iPP/Talc-NH_{2(g)}), by either gas or vapor processes, also show a plateau region similar to the exhibited by the neat iPP but shorter because of the shift up displacement of their β peaks. Otherwise, it is of interest to notice the strong shift up and larger α and β peaks observed in the G'' plot of the iPP/Talc-Cl/iPP-SA composite. These observations agree with both the larger size of the chlorine atom respecting to the hydroxyl group in the unmodified talc and the lower electro-negativity of the latter. Both effects should mean a decrease in the inter-atomic distances at the iPP/talc interphase and then of the interfacial ply thickness, showing the maximum interaction level with the SA groups grafted in the iPP-SA confined at the interface. The latter affects to the α' peak detection by the DMA spectrometer (Table III), being almost in the noise level if not evidenced in both the G'' plots of the iPP/iPP-SA and the iPP/iPP-SA/talc systems, as above discussed. According to this, both the G' and the G'' plots of the iPP/Talc-Cl/iPP-SA composite appear as the highest all along the temperature axis above the glass transition temperature. In the concerning to the aforementioned smoothing of the α peak with no evidence of any shoulder being assigned to any secondary crystallization entities (further the emergent plateau region in the G'' plots of both iPP/Talc-NH_{2(v)}/iPP-SA and iPP/Talc-NH_{2(g)}/iPP-SA), it is interesting to observe that once above the glass transition temperature both G'' curves almost overlap with those of iPP/Talc-NH_{2(v)} and iPP/Talc-NH_{2(g)}. It suggests any kind of saturation in the interfacial activity level above the glass transition temperature related to the chemisorption process of the talc modification.

However, below their respective glass transition peak, the presence of the iPP-SA increases greatly the maximum of the β peaks for both the iPP/Talc-NH_{2(v)}/iPP-SA and the iPP/Talc-Cl/iPP-SA. This indicates a higher population of "free" amorphous phase in the both sides of the interface modified composites than in the pristine one. Moreover, a remarkable difference is appreciated in the G'' plot of the iPP/Talc-Cl/iPP-SA if compared with that without iPP-SA (iPP/Talc-Cl) that is almost similar to the pristine composite. By the comparison of both G'' plots it can be deduced that the iPP-SA as interfacial modifier was able to release just the same dissipation mechanisms for both of the mentioned composites showing a similar amount of "free" amorphous phase as main responsible of the glass transition, otherwise, significantly higher than that of the pristine composite, and with a higher energetic threshold for the glass transition of each one of them with respect to the latter, 2°C above the β peak for the surface vapor phase aminated talc, and 6.5°C above for the chlorinated one, Table III. Another interesting observation is found on the G'' plot evolution of the iPP/Talc-NH_{2(g)} composites by comparison with the iPP/Talc-NH_{2(v)} composite. Meanwhile, below room temperature the iPP/Talc-NH_{2(v)} composite show increasing G'' values as temperature decreases giving rise to the expected maximum at the glass transition peak, the iPP/Talc-NH_{2(g)} composite G'' evolution does not fall once reached the maximum value but remains on an almost constant G'' value (the highest of all the studied

composites). The latter is evident in the first temperature zone where the dissipation capabilities are the lowest because to be restricted to that assigned to mere vibration motions. The comparison between the composites incorporating the chemisorption modified talc [Figure 3(B)] and those corresponding to the physisorption modified ones [Figure 3(C)] let make two observations confirming their differences (the chemisorption and the physisorption surface modified talc) from a DMA point of view. On one hand, that the G'' plots of the latter remain framed in the same response area that all the other composites studied (as expected) because of the finite dimensions of the interface. On the other hand, that all the curves (besides showing their respective β and α transition peaks) exhibit largest differences in the temperature range above their respective glass transition temperatures up to 60°C. This is the inflexion point where the G'' values evolve with positive slopes as temperature increases giving rise to the corresponding α peaks. Both solid symbols G'' curves on Figure 3(C) indicate that the presence of iPP-SA increased the interfacial interaction level between both the silane and the *n*-butyl-amine treated talc, but in different ways according the different structures of both modifiers. So, the latter shows a G'' curve similar but shift down with respect to that of the pristine composite, and a significant increase in the broadness of its glass transition peak. In contrast, the iPP/Talc-Silane/iPP-SA composite shows the broadest glass transition peak of all the composites studied, almost 10°C above that of the pristine composite, iPP/Talc (Table III). Once surpassed 60°C, the evolution is falling to converge with that of the pristine composite. This peak appears clearly overlapped with both the α and the α' peaks too. From these findings and since the DMA perspective, it can be concluded a much more homogeneous amorphous fraction involved in both the amorphous/crystal, and the iPP/treated talc interfacial regions for the modified composite that combines the iPP-SA and the silane treated talc (iPP/Talc-Silane/iPP-SA), with an almost single energetic threshold (the largest of all the studied composites) which seems to involve all the amorphous regions wherever they were placed. Below the glass transition temperature, the iPP/Talc-Silane/iPP-SA shows G'' values approaching to those of the pristine one. At even below temperature (between -20 and -10°C) this composite exhibits values very similar to those of iPP/Talc-*n*BuNH₂/iPP-SA. It is important to notice the breathing of its glass transition peak 4°C lower than that of the pristine composite (Table III) which agrees with the lower electro-negativity of the *n*-butyl amine treated talc surface.

Damping Behavior. Figure 4 displays the $\tan \delta$ plots of the composites studied in this article. The β transition peaks, which identify their corresponding glass transitions, are clearly observable in the second temperature region, and the peak values have been compiled in Table III. The molecular motions at the reinforcement/matrix interfacial region generally contribute to the damping response of the composites apart from those provided of each constituent. Hence, the increase of the interfacial volume is usually identified by an increase in the $\tan \delta$ peak width. We mainly consider here how the interfacial modifications may affect to the glass transition temperature. This is done by considering that the amorphous regions located at the

interfacial plies are affecting to both the amount and to the energy threshold of the cooperative movements of the chain segments located at the “free” amorphous phase able to give rise to the thermodynamic second-order transition that the glass transition represents.^{34,35}

Similarly to the previous discussions on G' and G'' , Figure 4(A) shows an almost symmetrical downward vertical shift of the $\tan \delta$ curve for the iPP/talc composite with respect to that for the neat iPP. This indicates the decrease in the phase out between both components of the complex modulus in the composite with a much more elastic response than that found for the neat iPP. At the first temperature region, the $\tan \delta$ values of the iPP/iPP-SA system almost overlap with those of iPP/talc confirming that even in such low amount (and in absence of the talc particles) the iPP-SA is detected as a foreign component by the DMA measurements. Meanwhile, the modified composite (iPP-talc/iPP-SA) is shown an upward shift $\tan \delta$ curve if compared with that of the neat iPP. Once in the second temperature zone (glass transition zone), it is remarkable the lower and almost similar peak areas for both the systems incorporating the iPP-SA. These shows glass transition temperatures of 6 and 11.5°C for the iPP/talc/iPP-SA and the iPP/iPP-SA compounds, respectively, and are above of those of both the pristine composite and the neat iPP (Table III). This evidence, on one hand, the decrease and almost similar amount of “free” amorphous phase yielding the glass transition in the compounds with iPP-SA. On the other hand, the upward shift energy threshold for the glass transition of both the iPP/talc/iPP-SA modified composite and the iPP/iPP-SA system. Once in the third temperature zone (between 40 and 80°C) all the $\tan \delta$ curves evolve by following very similar positive slopes with the exception of that of the iPP/iPP-SA system [Figure 4(A)]. This one begins to increase not before the 60°C and remains here in after as the lowest also in the next temperature region (between 80 and 140°C). In this zone and in contrast with the pristine composite and the neat iPP curves, the modified composite (iPP/talc/iPP-SA) shows constant $\tan \delta$ values between 100 and 130°C. The latter agrees with a higher elastic response of this composite than of the pristine one because of the increasing interactions between the talc surface and the polar groups grafted in the iPP-SA in the region temperature where the polymer macromolecules (and even more while much lower the molecular weight is) are greatly improved with respect to their ability to flow and thus to participate in the dissipative phenomena through long-range conformational changes. These findings agree with the isotactic grafted polypropylene used as interfacial modifier and its high conformational restriction level if compared with other grafted polypropylenes but atactic, used as interfacial modifiers as discussed elsewhere.^{30–33}

In the case of the modified composites based on the different chemisorption modified talc [Figure 4(B)] it is confirmed the strongest interaction between the interfacial modifier and the surface gas aminated talc (iPP/Talc-NH_{2(g)}/iPP-SA) that shows the minimum amount of “free” amorphous phase to participate in the glass transition. At the same time its peak temperature (Table III) is almost the same than of the pristine composite (iPP/talc). In contrast, both the iPP/Talc-Cl/iPP-SA and the

iPP/Talc-NH_{2(v)}/iPP-SA composites show a glass transition upward shift respecting iPP/talc, but exhibiting significantly broader peak areas than the former. This is in agreeing with both the chemisorption process and the differences in size and electro-negativity of the chlorine atoms and the amine groups with respect to the original talc (with surface hydroxyl groups). Once in the third temperature zone, the $\tan \delta$ curve evolution of iPP/Talc-Cl/iPP-SA [in the same sense that G'' in Figure 3(B)] shows the lowest $\tan \delta$ values of all the composites studied at this work. This observation, jointly to the high glass transition temperature of this composite agrees with the expected increase in the interfacial thickness because of the presence of the iPP-SA as interfacial modifier plus, respectively, the 40% higher ionic radius of the chlorine than those of the hydroxyl, or amine groups, or the largest in molecular size physisorbed silane layer on the surface talc. The $\tan \delta$ plots corresponding to iPP/Talc-nBuNH₂/iPP-SA and iPP/Talc-Silane/iPP-SA [Figure 4(C)] shows interesting differences. In fact while iPP/Talc-nBuNH₂/iPP-SA shows a downward vertical shift respecting iPP/Talc-nBuNH₂, and so a decrease in the area below the glass transition peak (and then of the available “free” amorphous phase). This downward shift is also produced respecting that of the physisorbed treated talc composite with iPP-SA (iPP/Talc-Silane/iPP-SA) and even to the pristine composite (iPP/talc). In fact, iPP/Talc-Silane/iPP-SA showed the highest upward vertical shift of the $\tan \delta$ plots of all the studied composites also evidenced by a significant widening of the glass transition peak. The first effect should indicate the poorer interface adhesion of all the composites studied, while the latter suggests molecular relaxations in iPP/Talc-Silane/iPP-SA that were not present in iPP/Talc and iPP/Talc-nBuNH₂/iPP-SA. This is identifying the highest disturbed amorphous phase of all the studied composites,¹³ and agrees with the highest constraints at the amorphous/crystal interface imposed to those semicrystalline iPP-SA chains located at the talc/iPP matrix interphase caused by the molecular size of the silane moieties (the largest of all the compounds studied).

Glass Transition Temperature Criteria

It is known that the upward shifts of the glass transition peak are associated to a mobility decrease of the “free” amorphous phase in the polymer. From the perspective of the DMA spectra and because of the frequency dependence of the records, it is also well accepted that the temperature at which the damping peak is located on each one of both the G'' and in the $\tan \delta$ plots is not coincident with that at which the real change in the thermodynamic property occurs. Further, and because of the different magnitude of that kinetic effect over the elapsed time necessary to reach a new equilibrium (while the temperature goes ahead on both the G'' and the $\tan \delta$ measurements) different values between their respective peak temperatures associated to the glass transition of the matrix are expected too. This is due to the natural relaxation times of each kind of chain segments on the amorphous regions and depends on they were located. In such sense, it is important to remember here the three well differentiated amorphous regions considered at this work, the bulk as “free” amorphous regions involved in the cooperative motions that the glass transition means and those

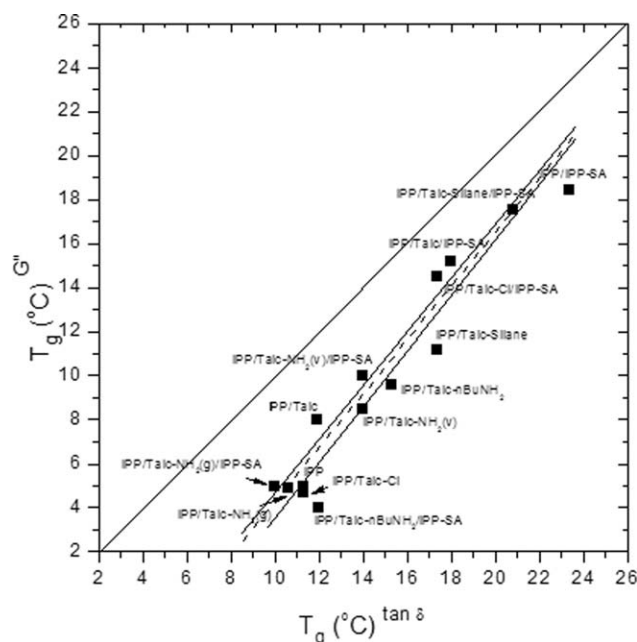


Figure 5. Glass transition peak values from G'' plots versus glass transition peak values from $\tan \delta$ plots.

two other located at the amorphous/crystal interfaces either in the bulk and the trans-crystalline regions.

Moreover, from early works^{21,23–26,34} it was well accepted the influence of the processing steps in the DMA responses of the semi crystalline polymers, and more specially in the above-mentioned different sensitivity to the kinetic effects between the G'' and the $\tan \delta$. The latter would be subject of the incoming works by authors. In advance, Figure 5 displays a double entry square plot showing the glass transition peak values obtained from the G'' curves of the different composites versus those obtained from the respective $\tan \delta$ curves. As it can be observed, never the diagonal of the square plot is crossed and always the glass transition peak temperatures, $\tan \delta$ measured, are higher than those coming from the G'' plots. Further and taking the square diagonal as reference, all the samples appear on an almost parametric downward shift straight line, which seems to approach to the diagonal as higher the glass transition peaks for the composites are, it means, as the corresponding composites approach to the extended glass transition model.³⁵ All the differences between the glass transition peaks from G'' and the $\tan \delta$ versus temperature curves are ranged between 2.8 and 6.6°C, being noteworthy that all the iPP-SA modified composites appear in the zone of the lowest differences, with the exception of those of the aminated (both physi or chemisorbed) modified talc. The latter could be assigned to the chemical reaction between some of the amine groups at the talc surface and the succinic anhydride groups grafted onto the iPP-SA chains. It is clear from these results, on one hand and beyond the improvement of the matrix/reinforcement polar affinities, the correlation with the interfacial volume availability depending on the molecular sizes of the moieties involved, which otherwise agrees with the finite dimension of the interface.³⁶ On the other hand, on the evidence that the DMA parameters results to be

sensitive to the different nature and extension of the interfacial modifications in the composite materials studied.

Glassy to Rubbery Transition Criteria

According different works,^{37,38} the efficiency of the reinforcements characterized by a preferential dimension and a well defined aspect ratio may be represented by a parameter (C). This parameter compares the behavior of the elastic component of the composite in the rubbery and the glassy state respecting the same for the polymer matrix. This parameter can be expressed as follows:

$$C = \frac{\left(\frac{G'_g}{G'_r} \right)_{\text{Composite}}}{\left(\frac{G'_g}{G'_r} \right)_{\text{iPP}}}, \quad (1)$$

where G'_g and G'_r are the storage modulus in the glassy and the rubbery regions, respectively. As usually G' decreases with temperature, it is expected that the G' values in the rubbery state were lower than those in the glassy state and so that the ratio (G'_g/G'_r) for the polymer matrix (iPP) throws always values higher than one. Hence, the higher the C values the lower the reinforcement efficiency. From G' plots displayed in Figures 2(A)–5(A), -10°C would be a reasonable temperature to take the G' values at the glassy state while 50°C has been considered as the reference temperature for the materials at the rubbery state. The values for the C parameter values have been compiled in Table III, being all of them lower than one, indicating that all the composites show a reinforcing effect respecting to the pristine iPP. The effect of the semicrystalline character of the iPP matrix may be well differentiated by the C value for the iPP/iPP-SA system which shows that the C parameter as defined, results to be sensitive to the presence of this foreign component in the iPP matrix. This explains the lowest C value obtained for iPP/talc/iPP-SA respecting all the other composites. Also all the composites with iPP-SA show lower values than the same without iPP-SA, indicating the gain in efficiency provided by the presence of iPP-SA. As in our study we have used a series of composites with the same reinforcement content (Table II), we can use a standardized C parameter by comparing with the original iPP/talc rather than to the neat iPP. So, the new parameter obtained, C^* , will be expressed as follows:

$$C^* = \frac{\left(\frac{G'_g}{G'_r} \right)_{\text{Composite}}}{\left(\frac{G'_g}{G'_r} \right)_{\text{iPP/Talc}}}, \quad (2)$$

being $C^* = 1$, the value for the original pristine composite and according to the corresponding values compiled in Table III, almost all around 1.0, this approach seems to be not sensitive enough to the interfacial modifications in the composites.

Correlation with Macroscopic Properties

Table III includes the values for the elastic modulus obtained under tensile conditions (E) at room temperature for the indicated samples. These results match the results obtained by authors for equally formulated compounds.⁷ Also, this table includes the values for the storage modulus (G') determined at the same conditions. Figure 6 plots the values of the storage modulus (G') versus the tensile elastic modulus (E) measured at room temperature for all the indicated samples. So, an almost linear correlation of positive slope can be appreciated. It is

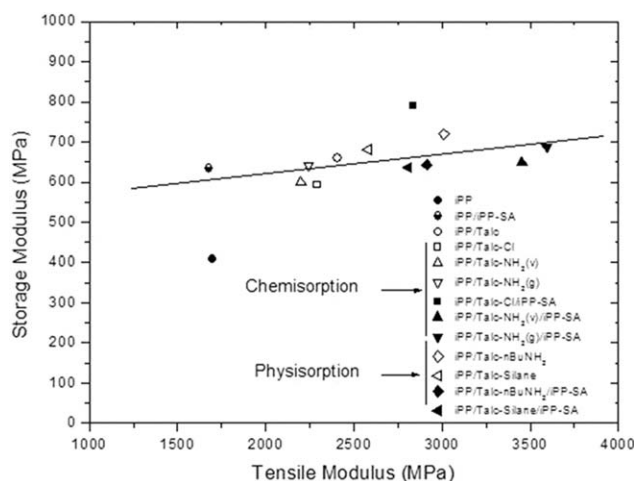


Figure 6. Storage modulus (G') versus tensile elastic modulus (E) for the indicated compounds measured at room temperature.

noteworthy to remark that this appears as different depending of the kind of surface treatment of the reinforcement. In fact, those incorporating chemisorbed talc (iPP/Talc- $\text{NH}_2(\text{v})$ and iPP/Talc- $\text{NH}_2(\text{g})$) and iPP/Talc-Cl) appears very close each other, due probably to the very similar nucleation effect induced (quite similar size of the bonded groups).¹³ However, when the composites incorporated the interfacial agent (iPP-SA), they increase notably the tensile elastic modulus. On the contrary, the composites with physisorbed talc (iPP-Talc-nBu NH_2 and iPP/Talc-Silane) exhibit a very different behavior due probably to the heterogeneous coating of the reinforcement particles. However, once iPP-SA is present in the composite the effect is to converge in the same area. The deviation of iPP/Talc-Cl/iPP-SA is probably related to the complexity of the interactions taking place due to the very different nature of the functionalities involved. Works trying to ascertain more about this aspect are in progress now. It is well worth to notice that the pristine iPP is outwards the (E , G') correlation while the iPP/iPP-SA system does although far from the composites E range but in the same than the pristine iPP as it was determined in previous works by authors.⁷

CONCLUSIONS

The interfacial changes performed in the iPP/talc system by different interfacial treatments have been monitored and proved by means of DMA. The study of the iPP/talc system at the 75 : 25, w/w, ratio (just in the reinforcement threshold of percolation for the reinforcement effects by the talc particles) by embracing five different temperature dependent relaxation zones, provides a comprehensive interpretation of the occurring phenomena that allow the researcher to establish a phenomenological criterion to follow the efficiency of the interfacial treatments proposed. The significant differences in both the elastic and the viscous responses of the composites have been assigned to the different interfacial modifications: from the matrix side, from the reinforcement side and from both. These mainly affecting to the glass, or β transition of the composites as well as to the possibility to record (or not) the α transition. The observed and discussed changes on both transition regions full agree with the already established fact that

the semicrystalline interfacial modifier agent is rejected from the pristine matrix due to their polar moieties. The results obtained are coherent with the fact that the polar moieties (succinic anhydride) are always rejected from the crystalline structures²⁹ and placed at the largest constrained surroundings of the amorphous iPP/talc interphase as published by authors elsewhere.^{30–33,39} The isotactic sequences linked by primary bond to the polar groups embedded in these amorphous regions yield secondary crystallization processes, more or less affected by the surface talc, which varies from the original one, up to those of the physisorbed, or chemisorbed modified talc borders. The criteria based on the composite to matrix ratio between the ratio between the glassy and rubbery storage modulus (C and C^* constants) provide a valuable but not enough sensitive information to obtain a holistic correlation between the dynamic mechanical behavior of the composites and the different interfacial modifications performed. The preliminary correlation found between the macroscopic elastic tensile modulus (E) and the elastic component of the complex modulus (G') at room temperature shows a coherent variation range for both mechanical parameters that are linked to the different interfacial modifications on the composites. The latter needs of further investigations concerning the influence of the processing steps. This will be the aim of forthcoming papers. In this sense, it is noteworthy to establish that once significant interfacial changes have been ascertained by macroscopic means, they must be (and are) found and detected by microscopic scale parameters, while the contrary is not true.

REFERENCES

1. Stamhuis, J. E. *Polym. Compos.* **1983**, *5*, 202.
2. Stamhuis, J. E. *J. Appl. Polym. Sci.* **1988**, *9*, 72.
3. Rybnikar, F. *J. Appl. Polym. Sci.* **1989**, *38*, 1479.
4. Rybnikar, F. *Eur. Polym. J.* **1991**, *27*, 549.
5. Fujiyama, M.; Wakino, T. *J. Appl. Polym. Sci.* **1991**, *42*, 9.
6. Karger-Kocsis, J. *Polypropylene. Structure, Blends and Composites*; Chapman & Hall: London, **1995**.
7. Taranco, J.; Laguna, O.; Collar, E. P. *J. Polym. Eng.* **1992**, *11*, 325.
8. Taranco, J.; Laguna, O.; Collar, E. P. *J. Polym. Eng.* **1992**, *11*, 335.
9. Taranco, J.; Laguna, O.; Collar, E. P. *J. Polym. Eng.* **1992**, *11*, 345.
10. Taranco, J.; Laguna, O.; Collar, E. P. *J. Polym. Eng.* **1992**, *11*, 359.
11. Taranco, J.; García-Martínez, J. M.; Laguna, O.; Collar, E. P. *J. Polym. Eng.* **1994**, *13*, 287.
12. Pukánszky, B. *Eur. Polym. J.* **2005**, *41*, 645.
13. García-Martínez, J. M.; Taranco, J.; Collar, E. P. *J. Appl. Polym. Sci.* **2009**, *114*, 551.
14. García-Martínez, J. M.; Taranco, J.; Areso, S.; Collar, E. P. *Res. Rev. Mat. Sci. Chem.* **2014**, *4*, 35.
15. García-Martínez, J. M.; Taranco, J.; Areso, S.; Collar, E. P. In *Polyolefin Blends*; Kyu, T.; Nwabunma, D., Eds.; Wiley: New Jersey, **2008**; Chapter 13, p 379.
16. Feng, Q.; Wang, M.; Yongbo, H.; Guo, S. *Compos. A: Appl. Sci. Manufact.* **2014**, *58*, 7.
17. Wang, K.; Bahlouli, N.; Addiego, F.; Aszi, S.; Remond, Y.; Ruch, D.; Muller, R. *Polym. Deg. Stabil.* **2013**, *98*, 1275.

18. Castillo, L. A.; Barbosa, S. E.; Capiati, N. J. *Polym. Eng. Sci.* **2013**, *53*, 89.
19. Castillo, L. A.; Barbosa, S. E.; Capiati, N. J. *J. Appl. Polym. Sci.* **2012**, *126*, 1763.
20. Brandup, J.; Himergut, E. *Polymer Handbook*, 3rd ed.; Wiley: New York, **1989**.
21. Wunderlich, B. *Thermal Analysis*; Academic Press: San Diego, **1990**.
22. Nielsen, L. E. *Mechanical Properties of Polymers and Composites*; Marcel Dekker: New York, **1974**.
23. Akay, M. *Compos. Sci. Technol.* **1993**, *47*, 419.
24. Grein, C.; Bernreiner, H.; Gahleitner, M. *J. Appl. Polym. Sci.* **2004**, *93*, 1854.
25. Sepe, M. P. *Dynamic Mechanical Analysis for Plastic Engineering*; PDL Handbook Series: Norwich, New York, **1998**.
26. Phan, T. T. M.; De Nicola, A. J.; Schadler, L. S. *J. Appl. Polym. Sci.* **1998**, *68*, 1451.
27. Calvert, P. D.; Ryan, T. G. *Polymer* **1978**, *19*, 611.
28. Collar, E. P.; Areso, S.; Laguna, O.; García-Martínez, J. M. *Eur. Polym. J.* **1999**, *35*, 1861.
29. Collar, E. P.; Cofrades, A. G.; Laguna, O.; Areso, S.; García-Martínez, J. M. *Eur. Polym. J.* **2000**, *36*, 2265.
30. García-Martínez, J. M.; Laguna, O.; Areso, S.; Collar, E. P. *Eur. Polym. J.* **2002**, *38*, 1583.
31. García-Martínez, J. M.; Laguna, O.; Areso, S.; Collar, E. P. *J. Appl. Polym. Sci.* **2001**, *81*, 625.
32. García-Martínez, J. M.; Laguna, O.; Areso, S.; Collar, E. P. *J. Polym. Sci. Polym. Phys.* **2002**, *40*, 1371.
33. Collar, E. P.; Cofrades, A. G.; Laguna, O.; Areso, S.; García-Martínez, J. M. *Eur. Polym. J.* **2003**, *39*, 157.
34. McCrum, N. G.; Read, B. E.; Williams, G. *Anelastic and Dielectric Effects in Polymeric Solids*; Wiley: London, **1967**.
35. Struik, L. C. E. *Polymer* **1987**, *28*, 1521.
36. Shadler, L. *Nat. Mater.* **2007**, *6*, 257.
37. Pothan, L. A.; Oommen, Z.; Thomas, S. *Compos. Sci. Technol.* **2003**, *63*, 283.
38. Marcovich, N. E.; Reboredo, M. M.; Aranguren, M. I. *J. Appl. Polym. Sci.* **1998**, *70*, 2121.
39. Ellis, G.; Marco, C.; Gómez, M. A.; Collar, E. P.; García-Martínez, J. M. *J. Macromol. Sci. Phys.* **2004**, *B43*, 253.